THE JOURNAL OF PHYSICAL CHEMISTRY B

ARTICLE

pubs.acs.org/JPCB

Effect of High Pressure on Fully Hydrated DPPC and POPC Bilayers

Rong Chen,[†] David Poger,[†] and Alan E. Mark*[,†,‡]

[†]School of Chemistry and Molecular Biosciences and [‡]Institute for Molecular Bioscience, The University of Queensland, Brisbane QLD 4072, Australia

ABSTRACT: Enhanced hydrostatic pressure can induce phase transitions in hydrated lipid bilayers especially those composed of saturated phospholipids. In this work, the phase behavior of fully hydrated DPPC (1,2-dipalmitoyl-*sn*-glycero-3-phosphocholine) and POPC (2-oleoyl-1-palmitoyl-*sn*-glycero-3-phosphocholine) bilayers as a function of pressure up to 3000 atm has been examined in atomic detail on time scales of up to 1.0 μs, using the molecular dynamics simulation technique. DPPC bilayers formed a rippled gel-like phase comprising a minor disordered fluid-like region and a major ordered gel-like region at 1000 atm, a partially interdigitated gel-like phase at 2000 atm, and a gel-like phase with most of the lipid acyl chains tilted with respect to the plane of the bilayer at 3000 atm. POPC bilayers formed a rippled gel-like phase at 1800, 2400, and 3000 atm. The phase behavior observed for both DPPC and POPC bilayers is in agreement with experiment. The simulations provide insight into the structural changes of DPPC and POPC bilayers as a function of pressure and demonstrate the ability to model biologically relevant lipid systems under high hydrostatic pressure.

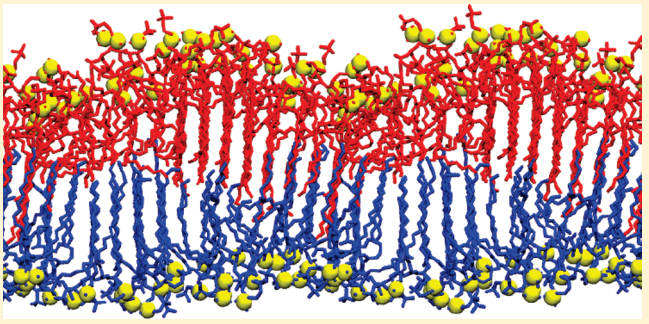

1. INTRODUCTION

Phospholipids, which form a primary component of cell membranes, can adopt a variety of phases in response to changes in external conditions, e.g., hydration level, hydrostatic pressure, temperature, and pH.[1] At ambient pressure, a lipid bilayer can adopt one of three main phases as a function of temperature and level of hydration namely, the Gel II ($L_{\beta'}$), the Gel I ($P_{\beta'}$, also known as the rippled gel phase), and the liquid-crystalline (L_α) phase. Of these, the L_α phase is the most biologically relevant. The transition from an $L_{\beta'}$ phase to a $P_{\beta'}$ phase is called the pretransition, while the transition from a $P_{\beta'}$ phase to an L_α phase is referred to as the main transition.[1]

To date most studies of lipid bilayers systems have focused on the effect of temperature and level of hydration, in part because experimental studies on the effect of hydrostatic pressure are difficult to perform. However, the importance of understanding high-pressure effects on lipid bilayers has long been recognized.[2] For example, hydrostatic pressure is able to reverse the effect of a range of general anesthetics that act on biological membranes, suggesting that these compounds may affect the fluidity or phase properties of lipid membranes.[3,4] High hydrostatic pressure has also been shown experimentally to elevate the main transition temperature of lipid bilayers.[5,6] In addition, high hydrostatic pressure can induce bilayers composed of saturated lipids, e.g., DMPC (1,2-dimyristoyl-*sn*-glycero-3-phosphocholine),[5] DPPC (1,2-dipalmitoyl-*sn*-glycero-3-phosphocholine),[7] and DPPG (1,2-dipalmitoyl-*sn*-glycero-3-phosphoglycerol),[8] to adopt a phase in which the structural properties of the bilayers are distinct from the three main phases ($L_{\beta'}$, $P_{\beta'}$, and L_α) at ambient pressure. In this pressure-induced phase, the lipid bilayer is significantly thinner than in a $P_{\beta'}$ or an $L_{\beta'}$ phase, and the lipid acyl chains are perpendicular as opposed to tilted with respect to the plane of the bilayer.[7] In addition, the lipid acyl chains appear more ordered than in a $P_{\beta'}$ or a $L_{\beta'}$ phase,[9] suggesting that an interdigitated gel phase ($L_{\beta i}$) is induced. For example, neutron diffraction studies have shown that at 326 K, DPPC bilayers form a gel phase at 1000 atm, and a $L_{\beta i}$ phase at 2000 atm.[7,10] ^{2}H NMR studies performed at 323 K have indicated that DPPC bilayers adopt a $P_{\beta'}$ phase at pressures between 750 and 1300 atm, an $L_{\beta i}$ phase at pressures between 1500 and 2000 atm, and an $L_{\beta'}$ phase at pressures between 2250 and 2750 atm.[9] Similar findings have been obtained in studies using other techniques.[11−13] Additional gel phases, e.g., Gel III, Gel IV, and Gel V, may also be induced in DPPC bilayers at pressures above 3000 atm.[11,13,14] Whereas a DPPC bilayer undergoes three phase transitions under increasing pressure up to 3000 atm and at temperatures above its main transition temperature of 315 K ($L_\alpha \rightarrow P_{\beta'}$, $P_{\beta'} \rightarrow L_{\beta i}$, and $L_{\beta i} \rightarrow L_{\beta'}$ or $L_{\beta i} \rightarrow$ Gel III),[9,11,13] bilayers composed of unsaturated lipids do not show the same response.[6,12] For example, no evidence of interdigitation in POPC (2-oleoyl-1-palmitoyl-*sn*-glycero-3-phosphocholine) bilayers under pressures up to 5000 atm has been observed.[6,12]

Although the available experimental evidence is consistent with the description of the phase behavior of DPPC bilayers as a function of pressure given above such as the formation of an interdigitated gel phase at 2000 atm and a temperature of 326 K, it is not possible to directly determine the exact structure of lipid bilayers in different phases in atomic detail using currently available experimental techniques. In particular, the molecular

Received: October 19, 2010
Revised: November 26, 2010
Published: December 31, 2010

structure of a lipid bilayer in the $P_{\beta'}$ phase is not well understood. Electron density profiles can give some indication of how the lipids pack within a bilayer, but at present high quality electron density profiles for a bilayer in the $P_{\beta'}$ phase are only available for DMPC.[15,16] These suggest that the bilayer in the $P_{\beta'}$ phase consists of a major thick region, M, and a minor thin region, m. However, critical aspects such as the conformation of the lipid acyl chains in the two regions cannot be observed directly. On the basis of the thickness of the bilayers, Nagle and co-workers among others have proposed that the M region represented a gel phase and the m region represented a fluid phase.[15,17] For example, the existence of fluid regions within a bilayer in the $P_{\beta'}$ phase is supported by wide-angle X-ray diffraction studies on DPPC bilayers.[17] Although it is not possible to directly observe the structure of lipids in a given phase experimentally, theoretical approaches such as molecular dynamics (MD) simulation techniques can be used to model structural changes within lipid bilayers associated with specific phase transitions. For example, Kranenburg et al. used a coarse grained model to examine the phase diagram of a DMPC bilayer as a function of temperature.[18] The simulations suggested that in the $P_{\beta'}$ phase, the DMPC bilayer consisted of a major gel-like region and a minor fluid like region,[18] in line with the earlier proposal of Nagle and co-workers.[15] de Vries et al. performed simulations using a united-atom model of a partially hydrated DPPC bilayer (23 waters/lipid) in which the temperature of the system was lowered from 323 to 283 K.[19] In these simulations, a major gel-like region and a minor fluid-like region formed initially.[19] However, on extending the simulations, the disordered region became fully interdigitated and gel-like.[19] The properties of the ripples such as the ripple length (λ_r = 12−16 nm), stacking repeat distance ($d \approx 6.5$ nm) and ripple amplitude ($A \approx 2.4$ nm) derived from these simulations[19] were considered to be in general agreement with the values derived from electron density profiles of DMPC bilayers in the $P_{\beta'}$ phase.[15] On the basis of this, the authors proposed that the bilayers, with an interdigitated m region, represented a $P_{\beta'}$ phase.[19] Similarly a fully interdigitated m region was observed in coarse-grained Monte Carlo simulations of a DPPC bilayer after cooling to T^* = 0.3 in reduced units.[20] However, the ripple wavelength ratio (M/m) was significantly higher than that found by de Vries et al.[19] In fact, experimental evidence suggests that the ripple length in $P_{\beta'}$ phase bilayers is not unique but varies depending on the external conditions. For example, two types of ripples with wavelengths of 13.0−14.4 nm and 25.5−33.0 nm were observed in the same DPPC bilayer by X-ray diffraction.[21] This was confirmed in subsequent studies using atomic force microscopy in which three types of ripples with wavelengths of 15, 28, and ∼55 nm were found in different regions of the same bilayer.[22] Thus the period of the ripples within lipid bilayers in the $P_{\beta'}$ phase appears to be sensitive to various external conditions, such as the temperature and the heating or cooling protocol used in the experiment.[21,23] For example, according to X-ray diffraction data, DPPC bilayers in the $P_{\beta'}$ phase with distinct ripples were formed by heating the bilayer from the $L_{\beta'}$ phase or cooling from the L_α phase.[21] Thus despite extensive effort both experimentally and theoretically, the exact structure of lipid bilayers in the $P_{\beta'}$ phase is yet to be fully resolved.

Here, an MD simulation study focusing on the phase behavior of fully hydrated DPPC and POPC bilayers as a function of pressure is presented. This work provides insights into the structural changes associated with increasing pressure in atomic detail, as well as demonstrating the ability of the GROMOS 54a7 force field for lipids[24] to reproduce the effect of high hydrostatic pressure in these systems.

2. METHODS

2.1. Simulation Details. All simulations were performed using the GROMACS simulation program version 3.2.1.[25] The GROMOS 54a7 force field for lipids which incorporates the changes proposed by Poger et al.[24] was used to describe the lipids. The solvent water was described using the SPC (simple point charge) water model.[26] Rectangular periodic boundary conditions were applied. Both the temperature and the pressure of the system were maintained close to the reference values using the Berendsen weak coupling method.[27] Time constants of 0.1 and 1.0 ps were used for the temperature and pressure coupling, respectively. Unless indicated otherwise, the pressure coupling was semi-isotropic. The LINCS[28] algorithm was used to constrain the length of all bonds within the lipids. The geometry of water was constrained using SETTLE.[29] In order to extend the time scale that could be simulated, the mass of the hydrogens in water was increased (4 amu) and the mass of the oxygen was decreased (10 amu) accordingly. This eliminates high frequency librations in water, allowing a time step of 5 fs to be used to integrate the equations of motion without significantly affecting thermodynamic properties of the system.[30,31] Nonbonded interactions were evaluated using a twin-range cutoff scheme. Interactions within the short-range cutoff of 0.8 nm were calculated every time step, while interactions between 0.8 and 1.4 nm were updated every two steps together with the pair list. A reaction-field correction[32] was applied to correct for the truncation of the electrostatic interactions beyond 1.4 nm. The relative dielectric permittivity of the medium (mainly the SPC water) outside the cutoff of 1.4 nm was set to 62.[33]

The initial structures of a DPPC bilayer (64 lipids/leaflet, 5841 water molecules) and a POPC bilayer (64 lipids/leaflet, 5941 water molecules) were obtained from equilibrated simulations of lamellar DPPC and POPC bilayers in a L_α phase as described by Poger et al.[24,34] Initial structures of two DPPC bilayers with 256 lipids/leaflet were constructed by replicating the structure of the DPPC bilayer after 120 ns of simulation at 1 and 2000 atm in the x and y dimensions. The systems correspond to fully hydrated bilayers with the hydration level being above 30 waters/lipid.[35,36] The DPPC and POPC bilayers were simulated under pressures ranging from 1 to 3000 atm. The temperature was maintained constant at 326 K in the case of the DPPC bilayer and 300 K in the case of the POPC bilayer. As the main phase transition temperature is 315 K for DPPC[37] and 270 K for POPC[38] at ambient pressure, both bilayers should be in a L_α phase at 1 atm. The simulations performed are summarized in Table 1. Atomic coordinates were saved every 50 ps for analysis.

2.2. Data Analysis. The area per lipid, the thickness of the bilayer, the deuterium order parameters of the lipid acyl chains, and the degree of interdigitation (D_{int}) in a bilayer were calculated as follows. The area per lipid was computed as the lateral area of the simulation box divided by the number of lipids per leaflet. The thickness of the lipid bilayer was estimated as the difference between the average coordinates of the phosphorus atoms in each leaflet (P−P distance). The P−P distance obtained in simulations is comparable with the distance D_{HH} between the two

Table 1. Summary of the Simulations Performed

bilayer	label	lipids/leaflet	temperature (K)	pressure (atm)	total time (μs)
DPPC	DPPC-64−1	64	326	1	0.3
	DPPC-64−1000a[a]	64	326	1000	0.6
	DPPC-64−1000b[a]	64	326	1000	1.0
	DPPC-64−2000a[a]	64	326	2000	0.6
	DPPC-64−2000b[a]	64	326	2000	0.6
	DPPC-256−2000a[b,d]	256	326	2000	0.2
	DPPC-256−2000b[c,d]	256	326	2000	0.2
	DPPC-64−3000a[a]	64	326	3000	0.6
	DPPC-64−3000b[a]	64	326	3000	1.0
POPC	POPC-64−1	64	300	1	0.3
	POPC-64−1800a[a]	64	300	1800	0.6
	POPC-64−1800b[a]	64	300	1800	0.6
	POPC-64−2400[a]	64	300	2400	1.0
	POPC-64−3000[a]	64	300	3000	1.0

[a] Different initial structures were taken from the simulation DPPC-64−1 or POPC-64−1. [b] The initial structure was constructed by replicating one configuration from the simulation DPPC-64−1 in the x and y dimensions where the z axis is parallel to the bilayers normal. [c] The initial structure was constructed by replicating the configuration from the simulation DPPC-64−2000a at 0.12 μs in the x and y dimensions. [d] The pressure coupling was anisotropic.

main peaks in the electron density profile derived from X-ray diffraction studies.[39]

The deuterium order parameter (S_{CD}) was defined as follows:

$$S_{CD} = \frac{1}{2}\langle 3\cos^2\theta - 1\rangle$$

where θ is the angle between a specific carbon-deuterium bond and the bilayer normal.[40] The angular brackets denote an ensemble average. The GROMOS 54a7 force field is a united-atom force field in which aliphatic hydrogens are not treated explicitly but incorporated into the carbon to which they are attached. For this reason, the S_{CD} were derived based on the positions of the neighboring carbons assuming ideal geometries.[41] The first moment of the spectra (M_1) from ^{2}H NMR experiment[9] was converted to average $|S_{CD}|$ values according to the following formula:

$$M_1 = \frac{\pi}{\sqrt{3}}\frac{e^2qQ}{h}\overline{S_{CD}}$$

where e^2qQ/h = 167 kHz is the deuterium quadrupole coupling in a carbon-deuterium bond.[42]

The degree of interdigitation (D_{int}) was defined as follows:

$$D_{int} = \left\langle \frac{D_0 - D_1}{D_0} \right\rangle$$

where D_0 is the distance between a methyl carbon in the *sn*-1 lipid acyl chain and the phosphorus atom of the same lipid, D_1 is the minimum distance between the methyl carbon of lipids in a given leaflet and the phosphorus atoms from the lipids in the opposite leaflet. The angular brackets denote an ensemble average.

3. RESULTS AND DISCUSSION

3.1. General Properties. 3.1.1. DPPC. The average area per lipid and the thickness of the bilayer over the last 0.1 or 0.02 μs of each simulation are summarized in Table 2. Typical snapshots of the DPPC (64 lipids/leaflet) and POPC bilayers at different pressures after 0.3, 0.6, or 1.0 μs of simulation are shown in

Table 2. Average Area Per Lipid and the Bilayer Thickness (P−P distance) over the Last 0.02 or 0.1 μs of Each Simulation

label	sampling time (μs)	[a]area per lipid (nm^2)	[a]bilayer thickness (nm)
DPPC-64−1	0.1	0.63	3.67
DPPC-64−1000a	0.1	0.60	[b]4.04
DPPC-64−1000b	0.1	0.55	[b]4.35
DPPC-64−2000a	0.1	0.54	[c]2.94
DPPC-64−2000b	0.1	0.54	[c]3.00
DPPC-256−2000a	0.02	0.56	3.78
DPPC-256−2000b	0.02	0.54	3.86
DPPC-64−3000a	0.1	0.53	3.83
DPPC-64−3000b	0.1	0.54	3.76
POPC-64−1	0.1	0.62	3.83
POPC-64−1800a	0.1	0.58	3.76
POPC-64−1800b	0.1	0.58	3.83
POPC-64−2400	0.1	0.56	3.86
POPC-64−3000	0.1	0.56	3.77

[a] The values represent an average over the last 0.1 μs (2000 frames) or 0.02 μs (400 frames) in each simulation. The standard error was <0.001 in all cases. [b] The value is that of the gel-like region. [c] The value is that of the interdigitated region.

Figure 1. At 1 atm, the acyl chains of DPPC are disordered (Figure 1A). The average thickness of the DPPC bilayer was 3.67 nm in the simulation DPPC-64−1, within 4% of the experimental value of 3.83 nm for a DPPC bilayer in a L_α phase at 1 atm.[39] At 1000 atm, the DPPC bilayer separated into a gel-like region and a disordered L_α-like region (Figure 1B). The thickness of the gel-like region was 4.04 and 4.35 nm in the simulations DPPC-64−1000a and DPPC-64−1000b, respectively. These values are comparable with the thickness of 4.42 nm for a DPPC bilayer in an $L_{\beta'}$ phase determined experimentally.[39] As noted previously, experimental studies of a bilayer in a $P_{\beta'}$ phase are consistent with the coexistence of gel-like and fluid-like regions.[15,17,22,43] For example, electron

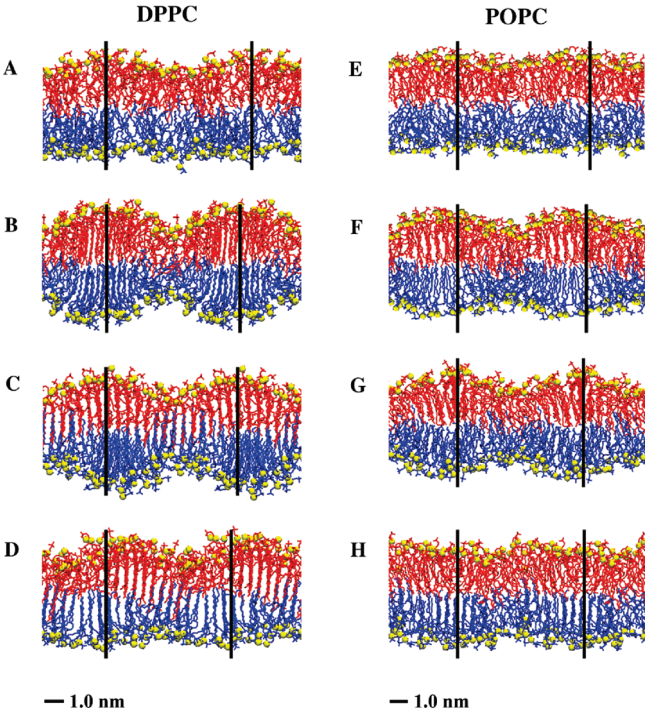

Figure 1. Snapshots of the DPPC bilayer simulated at 326 K after 0.3 μs of simulation at 1 atm (A), after 1.0 μs at 1000 atm (B), 0.6 μs at 2000 atm (C) and 1.0 μs at 3000 atm (D). Snapshots of the POPC bilayer simulated at 300 K after 0.3 μs of simulation at 1 atm (E), after 0.6 μs at 1800 atm (F), and 1.0 μs at 2400 atm (G) and 3000 atm (H). The phosphorus atoms in the lipid head groups are depicted as yellow spheres. The lipids in the two leaflets are shown in blue and red, respectively. Water molecules are not shown for clarity. Approximately two periodic boxes are shown. The size of the periodic unit is indicated in each case by the vertical lines.

density profiles of a DMPC bilayer suggest the presence of a major ordered *M* region and a minor disordered *m* region in the $P_{\beta'}$ phase. In this case, the *M* region has a similar thickness to a bilayer in the $L_{\beta'}$ phase while the thickness of the *m* region is similar to that of a bilayer in the L_α phase.[15] Note, the length of the acyl chains of DMPC and DPPC differ by just two CH_2 groups. Regions of distinct thickness in DPPC bilayers in a $P_{\beta'}$ phase have also been observed using atomic force microscopy. Again, the results suggest that the thinner and thicker regions correspond to a fluid and gel-like phase, respectively.[43] The coexistence of the ordered and disordered regions in the DPPC bilayer as observed in simulations DPPC-64−1000a and DPPC-64−1000b is consistent with the bilayer being in the $P_{\beta'}$ phase.

At 2000 atm, the regions of the DPPC bilayer that were disordered at 1000 atm became partially interdigitated with the acyl chains of the lipids lying perpendicular to the plane of the bilayer (Figure 1C). The average thickness of the interdigitated region was 2.94 nm in the simulation DPPC-64−2000a and 3.00 nm in the simulation DPPC-64−2000b, which compare favorably with the thickness of 2.94 nm for a DPPC bilayer in the $L_{\beta i}$ phase derived from neutron scattering density profiles.[7] In addition, the sharp symmetric peak observed in wide-angle neutron diffraction patterns of DPPC bilayers at 2000 atm and 323 K suggest that the acyl chains lie perpendicular to the plane of the bilayer in the $L_{\beta i}$ phase.[7] Thus, as the simulations reproduce, both the thickness and the orientation of the lipid acyl chains in the $L_{\beta i}$ phase, the DPPC bilayer in the simulations may be evolving into the $L_{\beta i}$ phase at 2000 atm.

It is important to note that as the systems were simulated under periodic boundary conditions, the period of the undulations in the membrane will by necessity be a multiple of the size of the box. As discussed above, wavelengths ranging from 13 to 55 nm have been proposed based on different experimental data. In order to be able to simulate the systems considered in this work on an extended time scale, the periodic repeat was set to approximately 6 nm. This is approximately half the wavelength of the minimal repeat observed experimentally. To investigate the effect of system size two additional simulations, DPPC-256−2000a and DPPC-256−2000b, were performed with 256 lipids/leaflet, which would allow a wavelength of 12 nm. In both cases, the ordered regions within the bilayer and orientation of the lipids remained similar to that illustrated in Figure 1C.

At 3000 atm, the interdigitated region was maintained. However, in contrast to that observed at 2000 atm (Figure 1C), the lipid acyl chains were tilted with respect to the plane of the bilayer (Figure 1D). The thickness of the DPPC bilayer in the noninterdigitated region was 4.30 nm in the simulation DPPC-64−3000a and 4.21 nm in the simulation DPPC-64−3000b, comparable with the experimental value of 4.42 nm for a DPPC bilayer in a $L_{\beta'}$ phase.[39] By calculating the ensemble average of the orientation of the vector formed by the second carbon of the lipid glycerol group and the geometric center of the lipid acyl chains with respect to the normal of the bilayer, the tilt of the lipid acyl chains, which were in a collinear arrangement, was determined to be ∼29.0°. This is in good agreement with the tilt of the acyl chains in DMPC (32.3°) and DPPC (31.6°) bilayers in the $L_{\beta'}$ phase derived from wide-angle X-ray scattering intensity data.[44,45] Therefore, the DPPC bilayer appears to be evolving into the $L_{\beta'}$ phase in the simulations at 3000 atm. Note, given the size of the systems and the fact that they had not yet evolved to a fully ordered state it was not possible to determine conclusively if the acyl chains were predominately tilted toward their nearest neighbor or their next nearest neighbors.[46]

3.1.2. POPC. At 1 atm, the POPC bilayer adopted a L_α phase. The average thickness of the POPC bilayer was 3.83 nm, which is comparable with the experimental value of 3.70 nm for a POPC bilayer in a L_α phase.[36] At 1800, 2400, and 3000 atm, the POPC bilayer formed a disordered L_α-like region and a more ordered gel-like region (Figure 1F− H). Experimental studies suggested that high hydrostatic pressure elevates the main phase transition temperature of POPC bilayers by 0.18−0.19 K/MPa.[6,47] In this case, increasing the pressure in the system from 1 atm to 1500−1600 atm would be expected to raise the main phase transition temperature from 270 K[38] to 300 K. Thus, at 300 K (the temperature at which the simulations of POPC were performed), a POPC bilayer would be expected to adopt a $L_{\beta'}$ phase at pressures ≥1600 atm. In the simulations, the complete transition from the L_α phase to the $L_{\beta'}$ phase was not observed. Rather, the final structures were similar to that of the DPPC bilayer at 1000 atm (Figure 1B). Thus, as discussed above in regard to DPPC, it is likely that POPC is adopting a $P_{\beta'}$ phase which is intermediate between the L_α and the $L_{\beta'}$ phases.

3.2. Acyl Chain Order. To provide a quantitative measure of changes in the degree of order within the acyl chains as a function of pressure, the deuterium order parameter $|S_{CD}|$ was computed as described in the Methods. Figure 2 shows the value of $|S_{CD}|$ averaged over all methylene hydrogens in the *sn*-1 palmitoyl chain of DPPC and POPC at different pressures as a function of the simulation time. For DPPC at 1 atm, the average value of $|S_{CD}|$ remains effectively constant at a value of approximately 0.17 indicating that the system is well equilibrated (Figure 2A). Note it has been shown previously

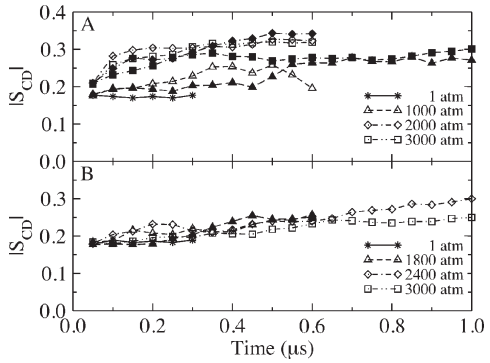

Figure 2. (A) The average deuterium order parameters ($|S_{CD}|$) of the *sn*-1 palmitoyl chain of DPPC (64 lipids/leaflet) as a function of the simulation time at 1 atm (*), 1000 atm (Δ), 2000 atm (◊), and 3000 atm (□). (B) The average $|S_{CD}|$ of the *sn*-1 palmitoyl chain of POPC as a function of the simulation time at 1 atm (*), 1800 atm (Δ), 2400 atm (◊), and 3000 atm (□). Note the filled symbols represent a second independent simulation.

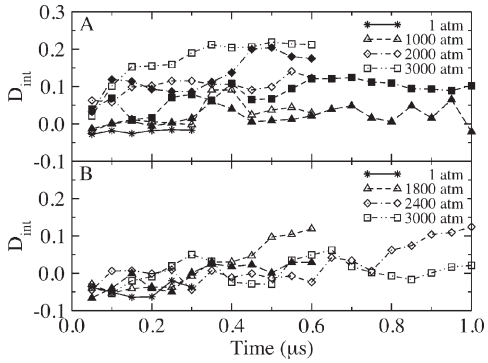

Figure 3. (A) The degree of interdigitation (D_{int}) in the DPPC bilayer with 64 lipids/leaflet as a function of the simulation time at 1 atm (*), 1000 atm (Δ), 2000 atm (◊), and 3000 atm (□). (B) The degree of interdigitation (D_{int}) in the POPC bilayer as a function of the simulation time at 1 atm (*), 1800 atm (Δ), 2400 atm (◊), and 3000 atm (□).

that using this model the values $|S_{CD}|$ are within 5−10% of the experimental values for each methylene group along the chain.[24,34] At 1000 atm, the average value of $|S_{CD}|$, while differing between the two simulations grew gradually reaching a value of 0.26 after 1.0 μs of simulation in DPPC-64−1000b or an increase of 0.09 over the value at 1 atm. At 2000 and 3000 atm, the average value of $|S_{CD}|$ rose rapidly during the first 0.1 μs and then grew steadily during the remainder of the simulation (Figure 2A). The average value of $|S_{CD}|$ increased by approximately 0.17 (after 0.6 μs) and 0.13 (after 1.0 μs) for the simulations performed at 2000 and 3000 atm, respectively. Deuterium order parameters for the methylene groups at positions 2, 9, and 13 in the palmitoyl chains of DPPC at 1000, 2000, and 3000 atm have been measured experimentally for a fully equilibrated membrane system by Peng et al.[9,42] These show an average increase over the values obtained at 1 atm of 0.22, 0.31, and 0.29 at 1000, 2000, and 3000 atm, respectively. Figure 2A shows that in the simulations, the DPPC bilayers at elevated pressure progressively become more ordered with time and even though the simulations are not yet fully equilibrated the trends observed experimentally are reproduced. In particular, the simulations predict that the average value of $|S_{CD}|$ at 3000 atm is lower than that at 2000 atm inline with differences in the first moment of the spectra (M_1) derived from ^{2}H NMR experiments.[9,42] This difference is generally interpreted as indicating that the acyl chains of DPPC are tilted with respect to the plane of the bilayer as is found in the simulations.[9,11,13,14]

In POPC, the average value of $|S_{CD}|$ at 1800, 2400, and 3000 atm also increases with simulation time (Figure 2B) in a similar manner to that observed in DPPC (Figure 2A). The average value of $|S_{CD}|$ for the *sn*-1 palmitoyl chain of POPC increased from 0.19 at 1 atm to approximately 0.25 after 0.6 μs at 1800, 2400, and 3000 atm. After 1.0 μs, the values were 0.3 and 0.25 for 2400 and 3000 atm, respectively. Note, for a bilayer system, in a given phase some increase in the degree of order within the acyl chains is expected as a function of pressure.[48,49] The deuterium order parameters also reflect changes in both the local and long-range order of the lipids linked to any associated phase transitions. Experimentally, the average value of $|S_{CD}|$ for POPC in a L_α phase increases by 1×10^{-4} MPa^{-1}.[49] Therefore, an increase in the average value of $|S_{CD}|$ of 0.02 would be expected on increasing the pressure from 1 to 1800 atm (∼180 MPa) if no phase transition was observed. The fact that an increase of approximately 0.06 was observed suggests that POPC is in fact adopting a more ordered phase in the simulations.

3.3. Interdigitation. Figure 3 shows the average degree of interdigitation (D_{int}) as a function of simulation time for the DPPC and POPC bilayers at each of the pressures investigated. The degree of interdigitation was estimated based on relative distance between the terminal carbon of the *sn*-1 acyl chain and the phosphorus atom of the same lipid compared to the closest phosphorus atom of a lipid in the opposite leaflet as described in the Methods. At 1 atm, the value of D_{int} for both POPC and DPPC varied between −0.1 and 0 indicating that the bilayers were not interdigitated. Note a negative value indicates that acyl chain is folded back upon itself. For DPPC at 1000 atm the value of D_{int} fluctuated between −0.05 and 0.1 suggesting the bilayer was not significantly interdigitated. In contrast, at 2000 and 3000 atm, the value of D_{int} is as large as 0.21 indicating that the bilayers are significantly interdigitated. For POPC at 1800, 2400, and 3000 atm, the values of D_{int} fluctuate between −0.1 and 0.1 suggesting that there was little persistent interdigitation.

4. CONCLUSIONS

In this work, molecular dynamics simulations have been used to investigate the structural properties of fully hydrated DPPC and POPC bilayers at various pressures ranging from 1 to 3000 atm. Starting from a DPPC bilayer in a L_α phase at 1 atm and 326 K, we observed a transition to a state consistent with a $P_{\beta'}$ phase at 1000 atm. At higher pressures we observed a further series of transitions consistent with the lipids adopting a $L_{\beta i}$ phase at 2000 atm and an $L_{\beta'}$ phase at 3000 atm. A schematic summarizing the initial state, the state observed in the simulations and the final states as inferred from experiment is shown in Figure 4. At 1000 atm, a DPPC bilayer is expected to adopt a $P_{\beta'}$ phase consisting of fluid-like and gel-like phase regions. The average thickness of the fluid-like and gel-like regions were in close agreement with experiment, as was the increase in the average value of $|S_{CD}|$. No significant interdigitation was observed at 1 atm. At 2000 atm, a partially interdigitated state in which the lipid acyl chains lay perpendicular to the plane of the bilayer was observed. This can be viewed as an intermediate in the transition to a fully interdigitated $L_{\beta i}$ phase. The thickness of the interdigitated region observed in the simulations is consistent with neutron scattering data and the increase in the average values of $|S_{CD}|$ is also consistent with the system beginning to adopt an $L_{\beta i}$ phase.

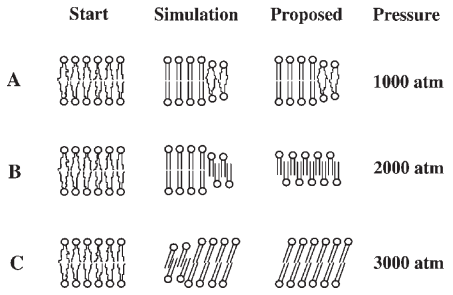

Figure 4. A schematic of the phase behavior of DPPC bilayers as a function of pressure. The column on the left shows the initial structure used in the simulation, the middle column the structure as observed in the simulations and the column on the right the structure proposed based on experiment. At 1000 atm (A) the bilayer adopts a $P_{\beta'}$ phase consisting of a major gel phase region and a minor L_α phase region. At 2000 atm (B) the bilayer adopted a partially interdigitated state in the simulations in which the lipid acyl chains lay perpendicular to the plane of the bilayer. The final state proposed is a fully interdigitated a $L_{\beta i}$ phase. At 3000 atm (C) the bilayer adopted a partially interdigitated state in the simulations in which the lipid acyl chains are tilted with respect to the plane of the bilayer. Experimentally, a tilted but noninterdigitated $L_{\beta'}$ phase has been proposed.

Finally, at 3000 atm a partially interdigitated state in which the lipid acyl chains were tilted with respect to the plane of the bilayer was observed. In this case, both the thickness and the angle of the tilt in the noninterdigitated region are consistent with a bilayer in the $L_{\beta'}$ phase.

Starting from a POPC bilayer in a L_α phase at 1 atm and 300 K, we observed an apparent transition to a $P_{\beta'}$ phase above 1800 atm with a disordered L_α-like region and a more ordered gel-like region. The increase in the average value of $|S_{CD}|$ with increasing pressure suggests that although still far from equilibrium, the POPC bilayers are gradually adopting a more ordered phase with limited interdigitation.

Overall, the simulations are in good agreement with a wide range of experimental studies shedding new light on the process by which lipid bilayers adjust to high hydrostatic pressure. The work also demonstrates the ability to model such systems under a range of pressure conditions using the GROMOS 54a7 force field for lipids.[24]

AUTHOR INFORMATION

Corresponding Author

*Tel.: +61 7 3365 4180; Fax.: +61 7 3365 3872; E-mail: a.e.mark@uq.edu.au.

ACKNOWLEDGMENT

This study was supported by the Australian Research Council (ARC) and made extensive use of the high performance computing resources of The University of Queensland and the National Computational Infrastructure (NCI) National Facility. R.C. thanks The University of Queensland for a PhD tuition fee waiver scholarship. A.E.M. is an ARC Federation Fellow.

REFERENCES

(1) Koynova, R.; Caffrey, M. *Biochim. Biophys. Acta* **1998,** *1376*, 91.
(2) Winter, R.; Jeworrek, C. *Soft Matter* **2009,** *5*, 3157.
(3) Lever, M. J.; Miller, K. W.; Paton, W. D. M.; Smith, E. B. *Nature* **1971,** *231*, 368.
(4) Wlodarczyk, A.; McMillan, P. F.; Greenfield, S. A. *Chem. Soc. Rev.* **2006,** *35*, 890.
(5) Ichimori, H.; Hata, T.; Matsuki, H.; Kaneshina, S. *Biochim. Biophys. Acta* **1998,** *1414*, 165.
(6) Ichimori, H.; Hata, T.; Matsuki, H.; Kaneshina, S. *Chem. Phys. Lipids* **1999,** *100*, 151.
(7) Braganza, L. F.; Worcester, D. L. *Biochemistry* **1986,** *25*, 2591.
(8) Singh, H.; Emberley, J.; Morrow, M. R. *Eur. Biophys. J.* **2008,** *37*, 783.
(9) Peng, X. D.; Jonas, A.; Jonas, J. *Biophys. J.* **1995,** *68*, 1137.
(10) Liu, N. I.; Kay, R. L. *Biochemistry* **1977,** *16*, 3484.
(11) Czeslik, C.; Reis, O.; Winter, R.; Rapp, G. *Chem. Phys. Lipids* **1998,** *91*, 135.
(12) Lee, B. S.; Mabry, S. A.; Jonas, A.; Jonas, J. *Chem. Phys. Lipids* **1995,** *78*, 103.
(13) Driscoll, D. A.; Jonas, J.; Jonas, A. *Chem. Phys. Lipids* **1991,** *58*, 97.
(14) Wong, R. T. T.; Siminovitch, D. J.; Mantsch, H. H. *Biochim. Biophys. Acta* **1988,** *947*, 139.
(15) Sun, W.-J.; Tristram-Nagle, S.; Suter, R. M.; Nagle, J. F. *Proc. Natl. Acad. Sci. U.S.A.* **1996,** *93*, 7008.
(16) Sengupta, K.; Raghunathan, V. A.; Katsaras, J. *Phys. Rev. E* **2003,** *68*, 031710.
(17) Rappolt, M.; Pabst, G.; Rapp, G.; Kriechbaum, M.; Amenitsch, H.; Krenn, C.; Bernstorff, S.; Laggner, P. *Eur. Biophys. J.* **2000,** *29*, 125.
(18) Kranenburg, M.; Laforge, C.; Smit, B. *Phys. Chem. Chem. Phys.* **2004,** *6*, 4531.
(19) de Vries, A. H.; Yefimov, S.; Mark, A. E.; Marrink, S.-J. *Proc. Natl. Acad. Sci. U.S.A.* **2005,** *102*, 5392.
(20) Lenz, O.; Schmid, F. *Phys. Rev. Lett.* **2007,** *98*, 058104.
(21) Katsaras, J.; Tristram-Nagle, S.; Liu, Y.; Headrick, R. L.; Fontes, E.; Mason, P. C.; Nagle, J. F. *Phys. Rev. E* **2000,** *61*, 5668.
(22) Kaasgaard, T.; Leidy, C.; Crowe, J. H.; Mouritsen, O. G.; Jørgensen, K. *Biophys. J.* **2003,** *85*, 350.
(23) Woodward, J. T., IV; Zasadzinski, J. A. *Biophys. J.* **1997,** *72*, 964.
(24) Poger, D.; van Gunsteren, W. F.; Mark, A. E. *J. Comput. Chem.* **2010,** *31*, 1117.
(25) van der Spoel, D.; Lindahl, E.; Hess, B.; Groenhof, G.; Mark, A. E.; Berendsen, H. J. C. *J. Comput. Chem.* **2005,** *26*, 1701.
(26) Berendsen, H. J. C.; Postma, J. P. M.; van Gunsteren, W. F.; Hermans, J. Interaction Models for Water in Relation to Protein Hydration. In *Intermolecular Forces*; Pullman, B., Ed.; D. Reidel: Dordrecht, The Netherlands, 1981; pp 331.
(27) Berendsen, H. J. C.; Postma, J. P. M.; van Gunsteren, W. F.; DiNola, A.; Haak, J. R. *J. Chem. Phys.* **1984,** *81*, 3684.
(28) Hess, B.; Bekker, H.; Berendsen, H. J. C.; Fraaije, J. G. E. M. *J. Comput. Chem.* **1997,** *18*, 1463.
(29) Miyamoto, S.; Kollman, P. A. *J. Comput. Chem.* **1992,** *13*, 952.
(30) Feenstra, K. A.; Hess, B.; Berendsen, H. J. C. *J. Comput. Chem.* **1999,** *20*, 786.
(31) Anézo, C.; de Vries, A. H.; Höltje, H. D.; Tieleman, D. P.; Marrink, S.-J. *J. Phys. Chem. B* **2003,** *107*, 9424.
(32) Tironi, I. G.; Sperb, R.; Smith, P. E.; van Gunsteren, W. F. *J. Chem. Phys.* **1995,** *102*, 5451.
(33) Heinz, T. N.; van Gunsteren, W. F.; Hünenberger, P. H. *J. Chem. Phys.* **2001,** *115*, 1125.
(34) Poger, D.; Mark, A. E. *J. Chem. Theory Comput.* **2010,** *6*, 325.
(35) Nagle, J. F.; Zhang, R.; Tristram-Nagle, S.; Sun, W.; Petrache, H. I.; Suter, R. M. *Biophys. J.* **1996,** *70*, 1419.
(36) Kučerka, N.; Tristram-Nagle, S.; Nagle, J. F. *J. Membr. Biol.* **2005,** *208*, 193.
(37) Huang, C. H.; Lapides, J. R.; Levin, I. W. *J. Am. Chem. Soc.* **1982,** *104*, 5926.
(38) Lewis, R. N. A. H.; Sykes, B. D.; Mcelhaney, R. N. *Biochemistry* **1988,** *27*, 880.
(39) Nagle, J. F.; Tristram-Nagle, S. *Biochim. Biophys. Acta* **2000,** *1469*, 159.
(40) Vermeer, L. S.; de Groot, B. L.; Réat, V.; Milon, A.; Czaplicki, J. *Eur. Biophys. J.* **2007,** *36*, 919.

(41) Egberts, E.; Marrink, S.-J.; Berendsen, H. J. C. *Eur. Biophys. J.* **1994,** *22*, 423.
(42) Davis, J. H. *Biochim. Biophys. Acta* **1983,** *737*, 117.
(43) Leidy, C.; Kaasgaard, T.; Crowe, J. H.; Mouritsen, O. G.; Jørgensen, K. *Biophys. J.* **2002,** *83*, 2625.
(44) Tristram-Nagle, S.; Liu, Y. F.; Legleiter, J.; Nagle, J. F. *Biophys. J.* **2002,** *83*, 3324.
(45) Sun, W.-J.; Suter, R. M.; Knewtson, M. A.; Worthington, C. R.; Tristram-Nagle, S.; Zhang, R.; Nagle, J. F. *Phys. Rev. E* **1994,** *49*, 4665.
(46) Katsaras, J.; Yang, D. S.; Epand, R. M. *Biophys. J.* **1992,** *63*, 1170.
(47) Skanes, I. D.; Stewart, J.; Keough, K. M. W.; Morrow, M. R. *Phys. Rev. E* **2006,** *74*, 051913.
(48) Driscoll, D. A.; Samarasinghe, S.; Adamy, S.; Jonas, J.; Jonas, A. *Biochemistry* **1991,** *30*, 3322.
(49) Brown, A.; Skanes, I.; Morrow, M. R. *Phys. Rev. E* **2004,** *69*, 011913.